THE MODULI SPACE OF SINGULAR GREAT CIRCLE FIBRATIONS OF S^3 AND THEIR DYNAMICS

Jingye Yang

A DISSERTATION

in

Mathematics

Presented to the Faculties of the University of Pennsylvania

in

Partial Fulfillment of the Requirements for the

Degree of Doctor of Philosophy

2023

Supervisor of Dissertation

Herman R. Gluck, Professor of Mathematics

Graduate Group Chairperson

Ron Donagi, Professor of Mathematics

Dissertation Committee

Herman R. Gluck, Professor of Mathematics
Dennis M. DeTurck, Professor of Mathematics
Mona Merling, Assistant Professor of Mathematics

THE MODULI SPACE OF SINGULAR GREAT CIRCLE FIBRATIONS OF S^3 AND THEIR DYNAMICS

Dedicated to the memory of my beloved grandfather, Lifa Wang, who always believed in my ability to be successful in my life.

ACKNOWLEDGEMENT

First of all, I would like to acknowledge and thank my advisor Herman Gluck. I am really grateful for the advice and help I have received from him in my whole Ph.D. career, as well as for his encouragement and concern for my life. I have learned so many things from collaboration with Herman including mathematics, teaching, writing, and living, and most importantly, how to become an excellent family member and friend.

Secondly, I would like to thank Mona Merling for her help and advice on my mathematics and how to develop a strong background in math and many other areas, as well as for infinitely many helpful conversations regarding school and life.

I also want to thank Dennis DeTurck for his generous support and guidance in my mathematical research and thesis projects. It is one of the best lessons I have ever learned to work together with him.

Moreover, I really thank Kai Wang for his supervision and support in my last year in the Ph.D. program. The hybrid life in both the math department and Wang's lab makes me competent in solving more difficult questions. In addition, without Kai's support, I couldn't imagine getting the postdoc fellowship.

My thanks to my friends and excellent colleagues Da Wu, Yi Wang, Tianyue Liu, Yidi Wang, Qingyun Zeng, and many others. You enriched my mathematical life in different ways. The department staff, Reshma Tanna, Monica Pallanti, Paula Scarborough, thank you very much for making my life much easier and taking care of many questions I had along the way.

My father Limin Yang and my mother Yi Wang and my grandparents, thank you so much for bearing with me, accompanying me, and loving me my entire life. My girlfriend Ruihui Zhang, thank you for taking care of me when I'm in help and contributing selflessly to our wonderful relationship.

I would like to finish by thanking my cutest family members with paws, Paopao, Huhu, Kiro and

Belo. You made my life much more colorful.

ABSTRACT

THE MODULI SPACE OF SINGULAR GREAT CIRCLE FIBRATIONS OF S^3 AND THEIR DYNAMICS

Jingye Yang

Herman R. Gluck

The Hopf fibrations of S^3 by great circles are one of the most important examples of the great circle fibrations of S^3, and have plenty of important geometric and topological features. The other great circle firbations of S^3 will deformation retract to the subspace of Hopf fibrations and thus has the homotopy type as $S^2 \cup S^2$. Among these great circle fibrations, only very few of them are differentiable. Starting from there, we expand the category of classic great circle fibrations of S^3 to the category of *general great circle fibrations of* S^2, containing classic great circle fibrations as its subspace and other fibrations called *singular great circle fibrations of* S^3. We will show that the moduli space of general great circle fibratioins have parellel properties as classic great circle fibrations. Specifically, the moduli space of general great circle can be characterized as weakly distance-decreasing maps between two unit S^2's with degree 0, while the classic great circle fibrations are corresponding to strictly distance-decreasing maps. We also visualize the formation of the *standard* singular fibration from a path of non-singular great circle fibrations starting from a Hopf fibration. In the end, we proved that the smooth great circle fibrations of S^3 are dense in the moduli space of general great circle fibrations of S^3.

TABLE OF CONTENTS

LIST OF ILLUSTRATIONS

CHAPTER 1

INTRODUCTION

1.1. Background

Think of a fiber bundle in which the fibers start to move around in the total space until some kind of singularity develops: perhaps some fibers bump into one another so that they are no longer disjoint, while other fibers may develop their own individual singularities. To separate these two phenomena from one another in a low-dimensional setting, we focus on fibrations of the three-sphere by great circles, and ask how these great circle fibers can move about within the three-sphere, until they first bump into one another. The advantage in starting this way is that we already know a concrete moduli space for the family of all smooth fibrations of the three-sphere by great circles: there are two components, according to right or left-handed screw sense, and a moduli space for each component is the family of all smooth mappings $f : S^2 \to S^2$ with $|df| < 1$ at each point. Each component deformation retracts to its subspace of constant maps, and these in turn correspond to the space of Hopf fibrations with given screw sense.

One kind of singularity formation is loss of differentiability while still remaining a continuous fibration ... not easily visible to the naked eye. But another kind of singularity formation is visually striking, with some great circle fibers intersecting their neighbors at a pair of antipodal points like longitudes meeting at the poles, while at the same time in a different location, other fibers are crossing one another like the many vapor trails of airplanes in the sky ... all happening in spite of this singular fibration being a limit of nonsingular smooth fibrations.

1.2. Organization

This thesis is organized in the following way. We will first introduce some definitions and lemmas which will be helpful for the rest of this work.

In Chapter 2, we will describe the structure of the oriented Grassmann manifold $\tilde{\mathrm{G}}_2\mathbb{R}^4$. Explicitly, we will show and prove two equivalent ways to characterize $\tilde{\mathrm{G}}_2\mathbb{R}^4$:

Theorem 1. Consider $\mathbb{R}^4$ as the space of quaternions, we will have two different correspondences of $\tilde{\mathrm{G}}_2\mathbb{R}^4$ as $S^2 \times \S^2$:

1. Consider an oriented 2-plane in $\mathbb{R}^4$ as a 2-algebra, then used the Hodge star operator to decompose the oriented Grassmannian $\tilde{\mathrm{G}}_2\mathbb{R}^4$

2. Directly map a 2-algebra $a \wedge b$ to $S^2 \times S^2$ via $(a^{-1}b, ba^{-1})$

and these two correspondences are identical.

This theorem helps us to understand the geometric structure of $\tilde{\mathrm{G}}_2\mathbb{R}^4$ and facilitate the proof of our main theorem in the following chapters.

In Chapter 3, we will give an overview of the moduli space of the great circle fibrations of S^3 and its homotopy type, following the argument by H. Gluck and F. Warner.

In Chapter 4, we will prove our first main theorem:

Theorem 2. The moduli space of all (non-singular or singular) great circle fibrations over S^3 is the closure of the moduli space of non-singular great circle fibrations of S^3 in the compact-open topology and consists of two connected components, each of which corresponds to the family of all continuous maps $f : S^2 \to S^2$ which

1. have degree zero and

2. are weakly distance-decreasing, that is, $d(f(x), f(y)) \leq d(x, y)$ for all $x, y \in S^2$.

With this main theorem, we will discover the dynamics of the continuous formation of a singular fibration from a path of (smooth) non-singular fibrations. This result will be elaborated with animation in Chapter 5. Meanwhile, we will prove the homotopy type of such moduli space of all great circle fibrations over S^3:

Theorem 3. Each component of this enlarged moduli space still deformation retracts to its subspace of constant maps, corresponding to the Hopf fibrations with a given screw sense so that it has the

homotopy type of the disjoint union of two copies of S^2.

In Chapter 6, inspired by the dynamics of a specific example in Chapter 5, we will prove a general "smooth approximation" result as our last main theorem:

Theorem 4. The smooth great circle fibrations of the three-sphere are dense in the continuous ones in the compact-open topology, and therefore dense in all great circle fibrations (singular or non-singular.)

CHAPTER 2

THE GRASSMANN MANIFOLD $\tilde{\mathrm{G}}_2\mathbb{R}^4$

2.1. Introuction

We will first give the definition of *Stiefel manifold*:

$$\mathrm{V}_k\mathbb{R}^n = \{(v_1, .., v_k)^T \mid v_i \in \mathbb{R}^n \text{ for } i = 1, ..., k \text{ is an orthonormal subset}\}$$

It has the induced topology as the subsapce of $\mathbb{R}^{kn}$. Notice that $O(n)$ acts on $\mathrm{V}_k\mathbb{R}^n$ smoothly and transitively with the isotropy subgroup $O(n-k)$, we know $\mathrm{V}_k\mathbb{R}^n \cong O(n)/O(n-k)$. If $k < n$, we also have $\mathrm{V}_k \cong SO(n)/SO(n-k)$. The general Grassmann manifold (also called Grassmannian) $\tilde{\mathrm{G}}_k\mathbb{R}^n$ is a space that consists of all oriented k-dimensional linear subspaces of the n-dimensional real vector space $\mathbb{R}^n$. We can define a quotient topology on it induced from the Stiefel manifold $\mathrm{V}_k\mathbb{R}^n$. Specifically, let

$$p \ : \ \mathrm{V}_k\mathbb{R}^n \ \mapsto \ \tilde{\mathrm{G}}_k\mathbb{R}^n$$

be the quotient map that takes the tuple of k orthonormal vectors to the oriented subspace spanned by these vectors. In addition, we can check that $\mathrm{V}_k\mathbb{R}^n \cong O(n)/O(n-k)$ as a lie group acts on $\tilde{\mathrm{G}}_k\mathbb{R}^n$ smoothly and transitively with the isotropy subgroup isomorphic to $SO(k)$, hence

$$\tilde{\mathrm{G}}_k\mathbb{R}^n \cong \mathrm{V}_k\mathbb{R}^n/SO(k) \cong O(n)/(O(n-k) \times SO(k))$$

and this shows that $\tilde{\mathrm{G}}_k\mathbb{R}^n$ is a homogeneous space. Similarly, we can define the (unoriented) Grassmannian $\mathrm{G}_k\mathbb{R}^n$ as the space of all k-dimensional linear subspaces of the n-dimensional real vector space $\mathbb{R}^n$, which is isomorphic to $O(n)/(O(n-k)\times O(k))$ as a smooth homogeneous manifold.

From this point forward, we will mainly focus on $\tilde{\mathrm{G}}_2\mathbb{R}^4$ or $\mathrm{G}_2\mathbb{R}^4$.

2.2. $\tilde{\mathrm{G}}_2\mathbb{R}^4 \cong S^2 \times S^2$ in two ways

We will show that $\tilde{\mathrm{G}}_2\mathbb{R}^4$ is isomorphic to $S^2 \times S^2$ in two different ways, using the exterior algebra or quaternions, both of which make important roles in the following chapters.

The exterior algebra $\bigwedge(V)$ of a vector space V over a field K (assume $\dim V = n$) is defined as the quotient algebra of the tensor algebra $T(V)$ by the two-sided ideal I generated by all elements of the form $x \otimes x$ for $x \in V$. The tensor product induced wedge product $x \wedge y = [x \otimes x]$ where $[x \otimes x]$ stands for the equivalent class of $x \otimes x$ in $\bigwedge(V) = T(V)/I$. It is also a graded algebra since

$$\bigwedge(V) = \bigwedge^0(V) \oplus \bigwedge^1(V) \oplus \cdots \oplus \bigwedge^n(V)$$

where $\bigwedge^k(V)$ is the kth exterior power of V defined as the vector subspace spanned by elements of the form:

$$v_1 \wedge v_2 \wedge \cdots \wedge v_k \ , \quad v_i \in V, \quad i = 1, 2, \cdots, k$$

We also call the element of $\bigwedge^k(V)$ a k-vector.

If V is a Euclidean space with an inner product, it induces the canonical inner product between decomposable k-vectors in $\bigwedge^k(V)$ as

$$\langle v_1 \wedge \cdots \wedge v_k, w_1 \wedge \cdots \wedge w_k \rangle = \det\big(\langle v_i, w_j \rangle\big),$$

and this is extended bilinearly to a non-degenerate inner product on $\bigwedge^k(V)$. We also treated it as a Riemannian manifold with this standard Euclidean metric. In the following discussion, We will only work with $\bigwedge^2(\mathbb{R}^4)$.

Let's define the subspace $W \subset \bigwedge^2(\mathbb{R}^4)$ of all decomposable 2-vectors $u \wedge v$ such that its length $\|u \wedge v\| = 1$, or equivalently (u, v) is an orthonormal basis of the plane they spanned. Then we can identify $\tilde{\mathrm{G}}_2\mathbb{R}^4$ with W in the following way: let $P \in \tilde{\mathrm{G}}_2\mathbb{R}^4$ be an oriented two-plane through the origin in $\mathbb{R}^4$, and u,v is an orthonormal basis for P ordered by its orientation, we have the association

$$P \leftrightarrow u \wedge v$$

Moreover, this association is actually a diffeomorphism, because $O(4)$ acts on W smoothly and transitively with the isotropy group $O(2) \times SO(2)$, and the association is equivariant with respect to this action. Notice that $\tilde{\mathrm{G}}_2\mathbb{R}^4$ has the induced geometry from this association as a Riemannian submanifold of $\bigwedge^2(\mathbb{R}^4)$. For this reason, we will use oriented 2-plane P or its associated decomposable unit 2-vector $\omega_P = u \wedge v$ interchangeably to represent an element of $\tilde{\mathrm{G}}_2\mathbb{R}^4$.

Let's denote e_1, e_2, e_3, e_4 the standard Euclidean basis of $\mathbb{R}^4$. The *Hodge star operator* $*$ is defined as the unique linear operator

$$* \ : \ \bigwedge^2(\mathbb{R}^4) \mapsto \bigwedge^2(\mathbb{R}^4)$$

such that

$$*(e_i \wedge e_j) = e_k \wedge e_l$$

where i, j, k, l is any permutation of $\{1, 2, 3, 4\}$ and $e_i \wedge e_j \wedge e_k \wedge e_l = e_1 \wedge e_2 \wedge e_3 \wedge e_4$. For example $*(e_1 \wedge e_2) = e_3 \wedge e_4$, $*(e_1 \wedge e_3) = -e_2 \wedge e_4$, etc.

Since $*$ is an involution and symmetric operator, it has two eigenvalues 1 and -1 associated with two orthogonal eigenspaces. Explicitly, H. Gluck and F. Warner proved that:

Theorem 2.2.1. $\bigwedge^2(\mathbb{R}^4)$ *has an orthogonal direct sum decomposition into two eigenspaces associated with the Hodge star* $*$*'s* 1 *and* -1 *eigenvalues.*

$$\bigwedge^2(\mathbb{R}^4) \ = \ E_- \oplus E_+$$
$$\omega = \frac{\omega - *\omega}{2} + \frac{\omega + *\omega}{2}$$

and we have 6 *fixed bais vectors*

$$b_1^- = \frac{e_1 \wedge e_2 - e_3 \wedge e_4}{2} \ , \ b_2^- = \frac{e_1 \wedge e_3 + e_2 \wedge e_4}{2} \ , \ b_3^- = \frac{e_1 \wedge e_4 - e_2 \wedge e_3}{2} \tag{2.1}$$

for E_-*,*

$$b_1^+ = \frac{e_1 \wedge e_2 + e_3 \wedge e_4}{2} \ , \ b_2^+ = \frac{e_1 \wedge e_3 - e_2 \wedge e_4}{2} \ , \ b_3^+ = \frac{e_1 \wedge e_4 + e_2 \wedge e_3}{2} \tag{2.2}$$

for E_+. They all have length $\frac{1}{\sqrt{2}}$ and are mutually orthogonal.
In addition, let S^2_- and S^2_+ denote the round 2-spheres of radius $\frac{1}{\sqrt{2}}$ centered at the origin in the eigenspaces E_- and E_+ respectively, then $\tilde{\mathrm{G}}_2\mathbb{R}^4$ as a subspace of $\bigwedge^2(\mathbb{R}^4)$ is exactly equal to $S^2_- \times S^2_+$.

This theorem gives a concrete geometric model of $\tilde{\mathrm{G}}_2\mathbb{R}^4$ as a product of two orthogonal 2-spheres with radius $\frac{1}{\sqrt{2}}$. Next, we will give another description of $\tilde{\mathrm{G}}_2\mathbb{R}^4$ with quaternions.

In the quaternion model, we identify $\mathbb{R}^4$ with the space of quaternions, namely $(a, b, c, d) \cong a + b\mathbf{i} + c\mathbf{j} + d\mathbf{k}$. (Notice that We will use (e_1, e_2, e_3, e_4) and $(1, \mathbf{i}, \mathbf{j}, \mathbf{k})$ interchangeably depending on the context (if we are using exterior algebra model or quaternion model)). Now we can directly define another diffeomorphism

$$\pi \ : \ \tilde{\mathrm{G}}_2\mathbb{R}^4 \mapsto S^2 \times S^2 \tag{2.3}$$

that maps the oriented plane P spanned by an orthonormal basis (u, v), to the point $(u^{-1}v, vu^{-1}) \in S^2 \times S^2$. Here "inverse" means the inverse of $u, v \in \mathbb{R}^4$ as a quaternion, which is equal to its conjugate $\bar{u}, \bar{v}$. Note that both of the coordinates

$$\pi_-(u, v) = u^{-1}v \ \text{ and } \ \pi_+(u, v) = vu^{-1}$$

are pure imaginary quaternions with the norm equal to 1. In fact, both left and right multiplication of a unit quaternion (u^{-1} in our case) are rotations of $\mathbb{R}^4$, taking the orthonormal basis (u, v) into the other orthonormal bases $(1, u^{-1}v)$ and $(1, vu^{-1})$. Therefore, both S^2's are the unit spheres in the subspace of pure imaginary quaternions (i.e. spanned by $\mathbf{i}$, $\mathbf{j}$ and $\mathbf{k}$).
It is useful to write down π's inverse. For a pair of pure imaginary quaternion (a, b). We have $\pi^{-1}(a, b) = \langle c, ca\rangle$ the oriented plane spanned by c and ca, where c is the midpoint of any geodesic arc connecting them on S^2. This can be confirmed through a simple computation, utilizing the fact that conjugation by a pure imaginary quaternion results in the rotation of the 2-sphere around that quaternion by π radians.

In the next section, we will prove that given suitable bases, these two models of $\tilde{\mathrm{G}}_2\mathbb{R}^4$ are identical, despite the different scales of geometry (the quaternion model has $\sqrt{2}$ times larger norm)

2.3. Equivalence of two models of $\tilde{\mathrm{G}}_2\mathbb{R}^4$

In this section, we will prove the following theorem

Theorem 2.3.1. *By matching the bases (5.2), (5.3) for exterior algebra model with the basis* $(\mathbf{i}, \mathbf{j}, \mathbf{k})$ *for the quaternion model, these two ways of* $\tilde{\mathrm{G}}_2\mathbb{R}^4 \cong S^2 \times S^2$ *are identical.*

Before we start the proof, let's define several notations for convenience and clarity. For any oriented plane $P \in \tilde{\mathrm{G}}_2\mathbb{R}^4$, assume its associated 2-vector $\omega_P = u \wedge v$ for an orthonormal frame $u, v \in P$. Then its exterior algebra model maps ω_P to $(\frac{\omega_P - *\omega_P}{2}, \frac{\omega_P + *\omega_P}{2}) \in S^2_- \times S^2_+$. It can be further written in the coordinate with respect to b_1^-, b_2^-, b_3^- and b_1^+, b_2^+, b_3^+. Namely,

$$\frac{\omega_P - *\omega_P}{2} = x_1 b_1^- + x_2 b_2^- + x_3 b_3^- \tag{2.4}$$

and

$$\frac{\omega_P - *\omega_P}{2} = y_1 b_1^+ + y_2 b_2^+ + y_3 b_3^+ \tag{2.5}$$

where $\sum_{i=1}^3 x_i^2 = \sum_{i=1}^3 y_i^2 = 1$. We will use $((x_1, x_2, x_3), (y_1, y_2, y_3))$ to represent the coordinate of P in the exterior algebra model in the proof.

In the quaternion model, $P = \langle u, v \rangle$ where u and v will be treated as two unit orthogonal quaternions. According to 2.3, $P = \langle u, v \rangle$ was mapped to $(u^{-1}v, vu^{-1}) \in S^2 \times S^2$. Under the basis $\mathbf{i}, \mathbf{j}, \mathbf{k}$ for both of S^2, it can be written as

$$u^{-1}v = \tilde{x}_1 \mathbf{i} + \tilde{x}_2 \mathbf{j} + \tilde{x}_3 \mathbf{k} \tag{2.6}$$

and

$$vu^{-1} = \tilde{y}_1 \mathbf{i} + \tilde{y}_2 \mathbf{j} + \tilde{y}_3 \mathbf{k} \tag{2.7}$$

where, similar to the case of the exterior algebra model, $\sum_{i=1}^3 \tilde{x}_i^2 = \sum_{i=1}^3 \tilde{y}_i^2 = 1$. We also use $((\tilde{x}_1, \tilde{x}_2, \tilde{x}_3), (\tilde{y}_1, \tilde{y}_2, \tilde{y}_3))$ as its coordinate in the quaternion's model. Then the theorem is equivalent

to say

$$((x_1, x_2, x_3), (y_1, y_2, y_3)) = ((\tilde{x}_1, \tilde{x}_2, \tilde{x}_3), (\tilde{y}_1, \tilde{y}_2, \tilde{y}_3)) \tag{2.8}$$

Proof. First, assume P passes through the real line (x-axis) and $P = \langle u, v\rangle = \langle 1, v\rangle$ or $\langle e_1, v\rangle$. In this case, $v = v_1e_2 + v_2e_3 + v_3e_4 = v_1\mathbf{i} + v_2\mathbf{j} + v_3\mathbf{k}$. Notice that

$$\begin{aligned} \omega_P &= 1 \wedge v \\ &= v_1e_1 \wedge e_2 + v_2e_1 \wedge e_3 + v_3e_1 \wedge e_3 \\ &= v_1(b_1^- + b_1^+) + v_2(b_2^- + b_2^+) + v_3(b_3^- + b_3^+) \end{aligned} \tag{2.9}$$

Therefore, $P = \omega_P$ has the coordinate $((x_1, x_2, x_3), (y_1, y_2, y_3)) = ((v_1, v_2, v_3), (v_1, v_2, v_3))$ in the exterior algebra model.

Now let's treat $1, v$ as quaternions and we have that

$$(1^{-1} \cdot v, v \cdot 1^{-1}) = (v, v) = (v_1\mathbf{i} + v_2\mathbf{j} + v_3\mathbf{k}, v_1\mathbf{i} + v_2\mathbf{j} + v_3\mathbf{k}) \tag{2.10}$$

This shows that P has the coordinate $((\tilde{x}_1, \tilde{x}_2, \tilde{x}_3), (\tilde{y}_1, \tilde{y}_2, \tilde{y}_3)) = ((v_1, v_2, v_3), (v_1, v_2, v_3))$ in the quaternion model. Therefore, 2.8 is true when P passes through the real line.

Now let's assume P is an arbitrary plane. We know that left and right multiplication of unit quaternion in $\mathbb{R}^4$ is equivalent to some rotation in $SO(4)$, we can define a quaternion action on a decomposable 2-vector by element-wise multiplication, i.e. $q \cdot (u \wedge v) = qu \wedge qv$ and expand linearly to all 2-vectors. Because of the definition and linearity, it's easy to check that this quaternion action commutes with the Hodge star automorphism $*$ on any 2-vectors. For example, $q \cdot (*(u \wedge v)) = *(q \cdot (u \wedge v))$.

Now, let u^{-1} act on $\omega_P = u \wedge v$, we have $u^{-1} \cdot \omega_P = 1 \wedge u^{-1}v$. Moreover, we can compute its

decomposition into $S^2_- \times S^2_+$ in the exterior algebra model as follows

$$\begin{aligned} u^{-1} \cdot \omega_P &= (\frac{u^{-1} \cdot \omega_P - *(u^{-1} \cdot \omega_P)}{2}, \frac{u^{-1} \cdot \omega_P + *(u^{-1} \cdot \omega_P)}{2}) \\ &= (\frac{u^{-1} \cdot \omega_P - u^{-1} \cdot (*\omega_P)}{2}, \frac{u^{-1} \cdot \omega_P + u^{-1} \cdot (*\omega_P)}{2}) \\ &= (u^{-1} \cdot \frac{\omega_P - *\omega_P}{2}, u^{-1} \cdot \frac{\omega_P + *\omega_P}{2}) \\ &= u^{-1} \cdot (\frac{\omega_P - *\omega_P}{2}, \frac{\omega_P + *\omega_P}{2}) \end{aligned} \tag{2.11}$$

The equation above suggests that we can first compute the coordinate of $u^{-1} \cdot \omega_P$ in the exterior model and then let u act on it to recover the coordinate of $\omega_P = (\frac{\omega_P - *\omega_P}{2}, \frac{\omega_P + *\omega_P}{2})$, which is our goal. Notice that the first and the third equations of 2.11 imply that E_- and E_+ are invariant subspaces under the action of left multiplication.

Assume that $u^{-1}v = k_1e_2 + k_2e_3 + k_3e_4$ or equivalently $= k_1\mathbf{i} + k_2\mathbf{j} + k_3\mathbf{k}$, then from previous argument for P passing through the real line, we know $u^{-1} \cdot \omega_P = (k_1b_1^- + k_2b_2^- + k_3b_3^-) + (k_1b_1^+ + k_2b_2^+ + k_3b_3^+)$. Therefore, we have

$$\omega_P = (k_1u \cdot b_1^- + k_2u \cdot b_2^- + k_3u \cdot b_3^-) + (k_1u \cdot b_1^+ + k_2u \cdot b_2^+ + k_3u \cdot b_3^+) \tag{2.12}$$

Therefore, we only need to compute the action of u on these 6 basis vectors $u \cdot b_i^-$ and $u \cdot b_i^+$ which is much simpler than directly computing ω_P's coordinate of the exterior model. This is the essence of using this group action. For convenience, we will denote $u = u_1 + u_2e_2 + u_3e_3 + u_4e_4$ or equivalently $= u_1 + u_2\mathbf{i} + u_3\mathbf{j} + u_4\mathbf{k}$ in the following computatioin.

Let's compute the first part of 2.12. Specifically, we have

$$\begin{aligned}
u \cdot b_1^- &= u \cdot \frac{e_1 \wedge e_2 - e_3 \wedge e_4}{2} \\
&= \frac{ue_1 \wedge ue_2 - ue_3 \wedge ue_4}{2} \\
&= \frac{(u_1e_1 + u_2e_2 + u_3e_3 + u_4e_4) \wedge (-u_2e_1 + u_1e_2 + u_4e_3 - u_3e_4)}{2} \\
&\qquad - \frac{(-u_3e_1 - u_4e_2 + u_1e_3 + u_2e_4) \wedge (-u_4e_1 + u_3e_2 - u_2e_3 + u_1e_4)}{2} \\
&= \frac{(u_1^2 + u_2^2 + u_3^2 + u_4^2)e_1 \wedge e_2 - (u_1^2 + u_2^2 + u_3^2 + u_4^2)e_3 \wedge e_4}{2} \\
&= \frac{e_1 \wedge e_2 - e_3 \wedge e_4}{2} \\
&= b_1^-
\end{aligned}$$

since $u_1^2 + u_2^2 + u_3^2 + u_4^2 = \|u\| = 1$.

We can compute the action on the other 5 basis vectors exactly in the same way, and have that

$$u \cdot b_i^- = b_i^-, \qquad \text{for } i = 1, 2, 3 \tag{2.13}$$

and

$$\begin{aligned}
&\begin{pmatrix} u \cdot b_1^+ & u \cdot b_2^+ & u \cdot b_3^+ \end{pmatrix} = \\
&\qquad \begin{pmatrix} b_1^+ & b_2^+ & b_3^+ \end{pmatrix} \begin{pmatrix} 1 - 2(u_3^2 + u_4^2) & 2(u_2u_3 - u_1u_4) & 2(u_2u_4 + u_1u_3) \\ 2(u_2u_3 + u_1u_4) & 1 - 2(u_2^2 + u_4^2) & 2(u_3u_4 - u_1u_2) \\ 2(u_2u_4 - u_1u_3) & 2(u_3u_4 + u_1u_2) & (1 - 2(u_2^2 + u_3^2)) \end{pmatrix}
\end{aligned} \tag{2.14}$$

We denote the rotation matrix in 2.14 as M_u.

With 2.13 and 2.14, we finally have the coordinate $((x_1, x_2, x_3), (y_1, y_2, y_3))$ of ω_P in the exterior algebra model:

$$\begin{aligned}
(x_1, x_2, x_3) &= (k_1, k_2, k_3) \\
(y_1, y_2, y_3) &= (k_1, k_2, k_3)\ M_u^T
\end{aligned} \tag{2.15}$$

Next, we will compute the coordinate $((\tilde{x}_1, \tilde{x}_2, \tilde{x}_3), (\tilde{y}_1, \tilde{y}_2, \tilde{y}_3))$ of ω_P in the quaternion model.

Remember that $P = \langle u, v \rangle$ in quaternion model with basis $\mathbf{i}, \mathbf{j}, \mathbf{k}$ is mapped to $(u^{-1}v, vu^{-1}) = (u^{-1}v, u(u^{-1}v)u^{-1}) = ((\tilde{x}_1, \tilde{x}_2, \tilde{x}_3), (\tilde{y}_1, \tilde{y}_2, \tilde{y}_3))$. The first entry $u^{-1}v$ equals $k_1\mathbf{i} + k_2\mathbf{j} + k_3\mathbf{k}$ thus has the coordinate $(\tilde{x}_1, \tilde{x}_2, \tilde{x}_3) = (k_1, k_2, k_3)$.

For the second entry, it is exactly the rotation of $\mathbb{R}^3$ by unit quaternion conjugation. Specifically, if we have $p = p_1\mathbf{i} + p_2\mathbf{j} + p_3\mathbf{k}$ in the 3-dimensional space considered as a quaternion with a real coordinate equal to zero, and $q = q_1 + q_2\mathbf{i} + q_3\mathbf{j} + q_4\mathbf{k}$ is a unit quaternion, then $p' = qpq^{-1} = p'_1\mathbf{i} + p'_2\mathbf{j} + p'_3\mathbf{k}$ is another vector in the 3-dimensional space by spatial rotation and can be computed with matrix multiplication as

$$\begin{pmatrix} p'_1 \\ p'_2 \\ p'_3 \end{pmatrix} = \begin{pmatrix} 1 - 2(q_3^2 + q_4^2) & 2(q_2q_3 - q_1q_4) & 2(q_2q_4 + q_1q_3) \\ 2(q_2q_3 + q_1q_4) & 1 - 2(q_2^2 + q_4^2) & 2(q_3q_4 - q_1q_2) \\ 2(q_2q_4 - q_1q_3) & 2(q_3q_4 + q_1q_2) & (1 - 2(q_2^2 + q_3^2)) \end{pmatrix} \begin{pmatrix} p_1 \\ p_2 \\ p_3 \end{pmatrix} \tag{2.16}$$

Now if we let $p = u^{-1}v$ and $q = u$, according to 2.16, we have

$$\begin{pmatrix} \tilde{y}_1 \\ \tilde{y}_2 \\ \tilde{y}_3 \end{pmatrix} = \begin{pmatrix} 1 - 2(u_3^2 + u_4^2) & 2(u_2u_3 - u_1u_4) & 2(u_2u_4 + u_1u_3) \\ 2(u_2u_3 + u_1u_4) & 1 - 2(u_2^2 + u_4^2) & 2(u_3u_4 - u_1u_2) \\ 2(u_2u_4 - u_1u_3) & 2(u_3u_4 + u_1u_2) & (1 - 2(u_2^2 + u_3^2)) \end{pmatrix} \begin{pmatrix} k_1 \\ k_2 \\ k_3 \end{pmatrix} \tag{2.17}$$

With 2.17, we finally have

$$\begin{aligned} (\tilde{x}_1, \tilde{x}_2, \tilde{x}_3) &= (k_1, k_2, k_3) \\ (\tilde{y}_1, \tilde{y}_2, \tilde{y}_3) &= (k_1, k_2, k_3)\ M_u^T \end{aligned} \tag{2.18}$$

Comparing (2.15) and (2.18), we come to the conclusion that these two models of $\tilde{\mathrm{G}}_2\mathbb{R}^4 \cong S^2 \times S^2$ are identical. □

CHAPTER 3

GREAT CIRCLE FIBRATIONS OF S^3

3.1. Introduction

In this chapter, we will breifly describe the results in the paper by Herman Gluck and Frank Warner, which discussed important properties of the moduli space of (non-singular) great circle fibrations of S^3.

Their work contains four main theorems:
What does an oriented great circle fibration of S^3 look like as a submanifold of $\tilde{\mathrm{G}}_2\mathbb{R}^4$? The answer is

Theorem 3.1.1 (Gluck and Warner)**.** *A submanifold of* $\tilde{\mathrm{G}}_2\mathbb{R}^4 \cong S^2 \times S^2$ *corresponds to a fibration* $\mathcal{F}$ *of* S^3 *by oriented great circles if and only if it is the graph of a distance decreasing map* f *from either* S^2 *factor to the other.*

Then, they discuss the smoothness property of $\mathcal{F}$ and its associated map f:

Theorem 3.1.2 (Gluck and Warner)**.** *The great circle fibration* $\mathcal{F}$ *is differentiable if and only if the corresponding distance decreasing map* f *is differentiable with* $|df| < 1$*. Inspired by the Borsuk-Ulam theorem, they showed*

Theorem 3.1.3 (Gluck and Warner)**.** *Any fibration of* S^3 *by great circles must contain some orthogonal pair of circles.*

At last, they prove the homotopy type of such moduli space

Theorem 3.1.4 (Gluck and Warner)**.** *The space of all oriented great circle fibrations of* S^3 *deformation retracts to the subspace of Hopf fibrations, and hence has the homotopy type of a pair of disjiont two-spheres.*

Since our work is closely related to the theorem 3.1.1, 3.1.2, and 3.1.4, we will give a quick review

on these results. We will refer to the paper by Herman Gluck and Frank Warner as [GSF] for convenience.

3.2. Non-singular great circle fibrations

in the paper [GSF], they rely on the first model of $\tilde{\mathrm{G}}_2\mathbb{R}^4 \cong S^2 \times S^2$ introduced in Chapter 2, where they treat each fiber as a 2-vector in $\bigwedge^2(\mathbb{R}^4)$.

In this model, a family of oriented great circle on S^3 will correspond to a subspace of $\tilde{\mathrm{G}}_2\mathbb{R}^4$. In general, this family of oriented circles will neither be disjoint from one another, nor will their union be all of S^3. So theorem 3.1.1 describes the submanifolds of the Grassmannian $\tilde{\mathrm{G}}_2\mathbb{R}^4$ which avoid these pitfalls, and hence represent oriented great circle fibrations of S^3. Namely, the corresponding subspace of $\tilde{\mathrm{G}}_2\mathbb{R}^4$ should be the graph of some distance decreasing map f from one S^2 to the other. But it doesn't answer how singularity of fibrations will develop as some fibers are bumped into each other or they never cover the whole S^3. We discuss this in rigorous details in Chapter 3, Chapter 4 and Chapter 5.

Based on this correspondence, they also notice that $\mathcal{F}$ is a smooth oriented great circle fibration of S^3, then the corresponding distance decreasing map f is also differentiable, and theorem 3.1.2 gives a necessary and sufficient statements between the smoothness of these two categories. However, we know there are plenty of non-differentiable distance-decreasing maps between round two-spheres. Hence there are plenty of non-differentiable great circle fibrations of S^3 as well. This encourges us to prove that the smooth ones are actually dense in the continuous ones in the open-compact topology. Details are in the chapter 6.

Finally, it is worthwhile to mention that the space of all Hopf fibrations (namely, translate the standard canonical Hopf fibration by an orthogonal matrix in $O(4)$) are corresponding to the constant maps f's from one S^2 to the other, and therefore a disjoint union of two copies of S^2.

3.3. Homotopy type of the moduli space

Since the family of Hopf fibrations are in the center of the all great circle fibrations of S^3 and they carry many good properties, they proved theorem 3.1.4 in the [GSF] that the moduli space of all

great circle fibrations will deformation retracts to the subsapce of Hopf fibrations, and thus the moduli space of all great circle fibrations has the homotopy type of $S^2 \cup S^2$. In the proof, they relied on the important result, "*Borsuk–Ulam theorem*", which implies the closed image of strictly distance-decreasing map $f : S^2 \mapsto S^2$ assoicated to a fibration $\mathcal{F}$ will be contained in a unique closed spherical cap.

We will show the same type of results for *general great circle fibrations* including singular ones. The proof has the similar flavor as the proof of theorem 3.1.4 but with different treatments using Borsuk–Ulam theorem. We will give the details argument in Chapter 4.

In the end, we want to emphasize again that we will treat the following objects as exactly **identical** through the whole work: an orineted 2-plane P, the oriented unit circle (fiber) $C \subset P$, a pair of orthonormal basis $\langle u, v \rangle \in P$ and a point of the oriented Grassmann manifold $\tilde{\mathrm{G}}_2\mathbb{R}^4$.

CHAPTER 4

SINGULAR FIBRATIONS OF S^3 BY GREAT CIRCLES

4.1. Introduction

In Chapter 3, we demonstrated that the moduli space of non-singular great circle fibrations of S^3 can be described as mapping spaces of strictly distance-dicreasing maps $f : S^2 \mapsto S^2$. In this chapter, we will enlarge our target category, and consider "*singular fibrations*" as well.

One envisions a great circle fibration within this moduli space where the fibers begin to shift within the total space until a singularity arises: perhaps some fibers bump into one another, so that they are no longer disjoint, while other fibers may develop their own individual singularities.

To separate these two phenomena from one another in a low-dimensional setting, we focus on the fibrations of the three-sphere by oriented great circles and investigate "how these great circle fibers can move about within the three-sphere until they **first** bump into one another". We call these fibrations "singular fibrations of S^3."

The advantage of starting this way is that we already know a concrete moduli space for the family of all continuous (smooth) fibrations of the three-sphere by oriented great circles: there are two components, according to right or left-handed screw sense, and a moduli space for each component is the family of all smooth mappings $f : S^2 \mapsto S^2$ with $\|df\| < 1$ at each point. If we are in the category of continuous fibrations instead of smooth fibrations, then "the family of all smooth mappings $f : S^2 \mapsto S^2$ with $\|df\| < 1$ at each point" will be loosened to "the family of all distance-decreasing mappings $f : S^2 \mapsto S^2$".

Based on this, we will give a rigorous argument of singular great circle fibrations of S^3 and the moduli space of all great circle fibrations (singular or non-singular). Explicitly, we will prove that:

Theorem 4.1.1. *The singular and non-singular great circle fibrations of the three-sphere correspond to two copies of the family of all continuous maps $f : S^2 \mapsto S^2$ which*

1. *has degree zero, and*

2. *are weakly distance-decreasing, that is,* $d(f(x), f(y)) \leq d(x, y)$ *for all* $x, y \in S^2$.

4.2. Enlarged moduli space of great circle fibrations of S^3 with singular fibrations

In this section, we will first introduce the definition of singular great circle fibrations and their topology. Later we will prove the main theorem presented in the Introduction section.

4.2.1. Singular great circle fibrations

Recall in Chapter 3, we learned that the moduli space of (non-singular) great circle fibrations of S^3 corresponds to two copies of all strictly distance-decreasing continuous maps $f : S^2 \to S^2$. let's call this moduli space $\mathcal{G}$. Moreover, it is endued with compact-open topology as a subspace of $C(S^2, S^2)$, the mapping space of all continuous maps on the two-sphere. Inspired by this result, we are able to consider a bigger picture of general great circle fibrations.

Definition 4.2.1. The moduli space of *general* great circle fibrations of S^3, denoted as $\mathcal{SG}$, is the closure of each component of the moduli space $\mathcal{G}$ (all continuous non-singular great circle fibrations of S^3) in the mapping space $C(S^2, S^2)$ with compact-open topology. Therefore, the singular fibrations are defined as those in the complement $\mathcal{SG} \setminus \mathcal{G}$.

Notice that for non-singular fibrations, its corresponding map $f : S^2 \mapsto S^2$ is strictly distance-decreasing, and then must have degree zero since its image can't be the whole S^2. Therefore, we hypothesize that for all general great circle fibrations, their associated maps will all have degree 0 and weakly distance-decreasing. This again leads to the main theorem of this Chapter.

It is useful to point out that the compact-open topology imposed on $C(S^2, S^2)$ is the same as the topology induced from the uniform metric $d(f, g) = \sup\{d(f(x), g(x)), x \in S^2\}$, since both S^2's are compact metric spaces. Therefore, any singular fibration can be approximated uniformly by a sequence of continuous non-singular fibrations in $\mathcal{G}$, or speaking equivalently, a sequence of strictly distance-decreasing maps.

4.2.2. Proof of main theorem

In this section, we will give detailed proof of the main theorem 4.1.1.

Proof. ("⇒") Given any singular great circle fibrations of S^3, called $\tilde{\mathcal{F}}$ with corresponding map $f : S^2 \to S^2$, by definition 4.2.1, it can be approximated uniformly (or in contact-open topology) by a sequence of continuous fibrations $\mathcal{F}_n \in \mathcal{G}$ with corresponding maps $f_n : S^2 \to S^2$. Therefore, we have

$$d(f_n(x), f_n(y)) < d(x, y), \tag{4.1}$$

for $x, y \in S^2$.

Moreover,

$$\begin{aligned} d(f(x),f(y)) &\leq d(f(x), f_n(x)) + d(f_n(x), f_n(y)) + d(f_n(y), f(y)) \\ &< d(f(x), f_n(x)) + d(x, y) + d(f_n(y), f(y)), \end{aligned} \tag{4.2}$$

Now let $n \to \infty$, we have

$$d(f(x), f(y)) \leq d(x, y) \qquad\qquad x, y \in S^2 \tag{4.3}$$

This proves the second neccesary condition of the theorem 4.1.1.

To show the degree of f is 0, we need to look at previous results from Chapter 3. By *Borsuk–Ulam theorem* we know the image of any $f_n \in \mathcal{G}$ of a continous great circle fibration will always stay in an open hemisphere. Since f can be approximated uniformly by f_n, f's image will also stay in an open disk of S^2 (we will show later it will stay in a closed hemisphere as well). This implies f is null-homotopic, and therefore has degree 0.

("⇐") In the other hand, given a weekly distance decreasing map with degree zero, we know it is null-homotopic by *Hopf Degree theorem*. To proceed, let's prove a lemma from *Borsuk–Ulam theorem*

Lemma. Every map $f : S^2 \to S^2$ which is null-homotopic must take a pair of antipodal points to the same image.

Proof: Proof by contradiction. If there exists a null-homotopic $f : S^2 \to S^2$ takes no antipodal pairs to the same image. Then for each pair of $x, -x \in S^2$, we will move points $f(x)$ and $f(-x)$, which are distinct, along the great circle generated by them at the same speed until they become a pair of antipodal points. If $f(x)$ already equal $-f(-x)$, they don't need to move. Specifically, if we imagine the sphere S^2 is center at the origin, then the homotopy H from f to the antipodal-preserving map g is defined as

$$H(x,t) = \frac{(1-t)f(x) + t(\frac{f(x)-f(-x)}{2})}{C} \tag{4.4}$$

where $C = \|(1-t)f(x) + t(\frac{f(x)-f(-x)}{2})\|$.

Now H takes f continuously to an antipodal-preserving map g. But we know from the classic *Borsuk–Ulam theorem* that this map g must have an odd degree, see [?] for details. Then f will also have an odd degree, which contradicts the assumption that f is null-homotopic which has a degree of zero. □

Now back to the proof of the main theorem. given a weekly distance decreasing map f with degree zero, it is null-homotopic and therefore by the lemma above, f must take a pair of antipodal points to the same image, say $f(x^*) = f(-x^*)$. Because f is weakly distance-decreasing, the image of f will be contained in a closed hemisphere centered at $f(x^*)$. Now, according to lemma 6.3.7, once we compress this hemisphere towards its center $f(x^*)$ by a ratio of $(1-\epsilon)$, it will immediately become a strictly distance-decreasing map . By shrinking ϵ, we can approximate uniformly f by a strictly distance-decreasing map, and this is exactly the definition of f representing a singular great circle fibration.

This completes the proof of the main theorem 4.1.1. □

4.3. Homotopy type of $\mathcal{SG}$

From theorem 3.1.4, we knew that the space of all oriented (non-singular) great circle fibrations of S^3 will deformation retracts to the subspace of Hopf fibrations. We will adpat the original proof in the [GSF] to show a strong results

Theorem 4.3.1. *The moduli space $\mathcal{SG}$ of general great circle fibrations of S^3 will deformation retracts to the subsapce of Hopf fibrations, and hence has the homotopy type of a pair of disjoint two-sphere.*

Proof. From the proof of theorem 4.1.1, we know that the map of f associated to a general great circle fibration $\mathcal{F}$ of S^3 (possibly singular) will take a pair of antipodal points, say x^* and $-x^*$ to the same image, and thus the whole image of f will be restrained in a closed hemisphere of centered at $f(x^*)$. However, this closed hemisphere may not be unique. For example, if the image of f is half of equator. We cannot use this hemisphere to construct a deformation retraction as in the paper [GSF].

Instead, let's look at the image $f(S^2)$ in S^2 and define its center of mass as

$$c = \int_{S^2} f(x)\, ds \tag{4.5}$$

where ds is the area form of S^2 such that the center c is weighted sum of position vector $f(x)$.
Notice that $f(S^2)$ is contained in some hemisphere, so c is far away from the origin. Hence, we can orthogonally project c back to the sphere and denote the projected point as c'. Namely, $c' = \frac{c}{\|c\|}$. Because the continuity of integral and norm function, c' varies continuously with respect to $f \in \mathcal{SG}$ with uniform metric.
Now let's shrink the image $f(S^2)$ along the geodesic towards the center c' until $f(S^2) \equiv c'$. Obviously the shrunk maps are still weakly distance-dicreasing with degree zero and thus represents a legit general great circle fibrations of S^3. This shrinking process is continuous as well. Since the final constant map is a Hopf fibration and all Hopf firations are fixed in the whole process, thus we define

a deformation retraction of $\mathcal{SG}$ to the subsapce of all Hopf Fibrations.

In the end, we have the homotopy type of $\mathcal{SG} \cong S^2 \cup S^2$. $\square$

CHAPTER 5

DYNAMICS OF SINGULARITY FORMATION

5.1. Introduction

In this chapter, we will compute a typical singular great circle fibration on S^3, which will be described below. We will call this singular fibration the "standard" one since it represents a good model for the family of general singular great circle fibrations on S^3 and has an inspiring visualization of its formation from a path of non-singular ones. We use those two different models of $\tilde{\mathrm{G}}_2\mathbb{R}^4$ introduced in Chapter 2 to achieve this. For consistency, we will follow the same notations and symbols in Chapter 2 unless otherwise stated.

Specifically, in the second section, we will use the exterior algebra model to compute the positions of fibers in the standard singular fibration. As a result, We will prove that

Theorem 5.1.1. *The standard singular fibration consists of two families of great circles:*

1. *"The red ones": all the great circles on S^3 which run through point 1. Most of them counted with only one orientation, except for those intersecting with the $\langle \mathbf{i}, \mathbf{j} \rangle$-plane, which counted with both orientations.*

2. *"The blue ones": all the great circles on $S^2(1, \mathbf{i}, \mathbf{j}) \subset S^3$ where $S^2(1, \mathbf{i}, \mathbf{j})$ means the unit two-sphere inside the space $\mathbb{R}^3$ spanned by $1, \mathbf{i}, \mathbf{j}$. Most of them are counted with only one orientation, except for those running through the point 1, which counted with both orientations.*

"The red ones" and "the blue ones" overlap on those great circle fibers with both orientations counted, and we call them "the orange ones".

Remark. We will give the definition of "red", "blue" and "orange" fibers in the following section.

In the third section, we will "visualize" how the non-singular great circle fibrations will continuously develop into the standard singular fibration. We will use the quaternion model to compute the

position of a specific fiber and stereographically project onto the $\mathbb{R}^3$ for visualization.

Before we give the definition of the standard singular fibration, let's first make some conventions. In either model (exterior algebra or quaternion) of $\tilde{\mathrm{G}}^2\mathbb{R}^4 \cong S^2_- \times S^2_+$, we will use "$-$" or "$+$" to represent the left or right two-sphere. According to theorem 2.3.1, since both of these two models are identical once we match their bases (5.2) and (5.3) for exterior algebra model with $(\mathbf{i}, \mathbf{j}, \mathbf{k})$ for quaternion model, we will always stick to this matching such that we can benefit from switching between these two models without interrupting the true underlying fibration. We will also follow the exact notation of (5.2) and (5.3) for the bases of the exterior algebra model and $(\mathbf{i}, \mathbf{j}, \mathbf{k})$ for the basis of the quaternion model. In addition, we will call the planes spanned by $\langle b_1^-, b_2^+\rangle$, $\langle b_1^+, b_2^+\rangle$ and $\langle \mathbf{i}, \mathbf{j}\rangle$ in S^2_- and S^2_+ "equatorial", and call b_3^-, b_3^+ and $\mathbf{k}$ the "north poles" lying in the "upper hemisphere" while $-b_3^-$, $-b_3^+$ and $-\mathbf{k}$ the "south poles" in the "lower hemisphere". This will help us visualize the dynamics in the following section.

Now let's give the definition of the standard singular fibration:

Definition 5.1.1. In either model (exterior algebra or quaternion) of $\tilde{\mathrm{G}}^2\mathbb{R}^4$ (there is no difference since the underlying fibration is identical), we define a "folding" map $f_s : S^2_- \mapsto S^2_+$ (from the left two-sphere S^2_- to the right two-sphere S^2_+), as follows:

$$f_s(x) = \begin{cases} x & \text{if } x \text{ in the upper hemisphere} \\ f_s(x^*) & \text{if } x \text{ in the lower hemisphere} \end{cases} \tag{5.1}$$

where x^* means the reflection through the equatorial circle. e.g., $\mathbf{i}^* = \mathbf{i}$, $\mathbf{j}^* = \mathbf{j}$, $\mathbf{k}^* = -\mathbf{k}$ (in the exterior algebra model); $(b_1^+)^* = b_1^+$, $(b_2^+)^* = b_2^+$, $(b_3^+)^* = -b_3^+$ (in the quaternion model), etc. Notice that here we identify S^2_- with S^2_+ via corresponding basis vectors (e.g. b_i^- to b_i^+, $\mathbf{i} \in S^2_-$ to $\mathbf{i} \in S^2_+$, etc).

Then the standard singular fibration is the fibration associated with this distance-decreasing map, denoted as $\mathcal{S}$.

5.2. Computation of the standard singular fibration

In this section, we will give an explicit algebraic expression of the standard singular fibration in the context of exterior algebra model. At the end, we will quickly mention how to reproduce the exact same results in the quaternion model, which confirms their equivalence again.

5.2.1. Singular fibers of the standard singular fibration

Recall that in Chpater 2, under the correspondence of an oriented plane P spanned by an orthonormal basis $\langle u, v\rangle \in P$ with the unit 2-vecotor $\omega_P = u \wedge v$, we show that $\tilde{\mathrm{G}}_2\mathbb{R}^4 \cong S^2_- \times S^2_+$, on which we fix two convex bases:

$$b_1^- = \frac{e_1 \wedge e_2 - e_3 \wedge e_4}{2} \ , \ b_2^- = \frac{e_1 \wedge e_3 + e_2 \wedge e_4}{2} \ , \ b_3^- = \frac{e_1 \wedge e_4 - e_2 \wedge e_3}{2} \tag{5.2}$$

on S^2_-,

$$b_1^+ = \frac{e_1 \wedge e_2 + e_3 \wedge e_4}{2} \ , \ b_2^+ = \frac{e_1 \wedge e_3 - e_2 \wedge e_4}{2} \ , \ b_3^+ = \frac{e_1 \wedge e_4 + e_2 \wedge e_3}{2} \tag{5.3}$$

on S^2_+. The decomposition of ω_P into these two spheres can be written as

$$\begin{aligned} \tilde{\mathrm{G}}_2\mathbb{R}^4 &\cong S^2_- \times S^2_+ \\ \omega &= \frac{\omega - *\omega}{2} + \frac{\omega + *\omega}{2} \end{aligned} \tag{5.4}$$

In Chapter 3 and Chapter 4, we showed how a general great circle fibration, as a submanifold of $\tilde{\mathrm{G}}^2\mathbb{R}^4$, corresponds to a weakly distance-decreasing map from either left S^2_- or right S^2_+ to the other one.

With all these backgrounds, We are able to compute each fiber of the standard singular fibration defined in the definition 5.1.1.

In the equation 5.1, we know the standard singular fibration has two components: one corresponds to the identity map on the upper hemisphere (called the "*red fibers*"), while the other corresponds

to the folding map of the lower hemisphere (called the "*blue fibers*"). These two components also intersect at the identity map on the equator (called the "*orange fibers*"). We will recover each of them from the graph of f_s to the fiberss of $\mathcal{S}$ as great circles in $S^3 \subset \mathbb{R}^4$

(1) "Red fibers"

Let's restrict f_s to the upper hemisphere $S^2_-\big|_U$ (we will use subscript "U" to mean "upper"), and consider any point $x \in S^2_-\big|_U$. We can expand x with respect to the basis

$$x = x_1 b_1^- + x_2 b_2^- + x_3 b_3^- \tag{5.5}$$

where $x_1^2 + x_2^2 + x_3^2 = 1$ and $x_3 \geq 0$.
According to the formula (5.1), we have

$$\begin{aligned} f_s(b_1^-) &= b_1^+ \\ f_x(b_2^-) &= b_2^+ \\ f_x(b_3^-) &= b_3^+ \end{aligned} \tag{5.6}$$

Combining (5.5) and (5.6), we get

$$f(x) = x_1 b_1^+ + x_2 b_2^+ + x_3 b_3^+ \tag{5.7}$$

Therefore, using formula (5.4), we can recover the original great circle fiber C_x corresponding to $(x, f(x))$ as

$$\begin{aligned} C_x &= x + f(x) \\ &= x_1 b_1^- + x_2 b_2^- + x_3 b_3^- + x_1 b_1^+ + x_2 b_2^+ + x_3 b_3^+ \\ &= x_1(\frac{e_1 \wedge e_2 - e_3 \wedge e_4}{2}) + x_2(\frac{e_1 \wedge e_3 + e_2 \wedge e_4}{2}) + x_3(\frac{e_1 \wedge e_4 - e_2 \wedge e_3}{2}) \\ &\quad + x_1(\frac{e_1 \wedge e_2 + e_3 \wedge e_4}{2}) + x_2(\frac{e_1 \wedge e_3 - e_2 \wedge e_4}{2}) + x_3(\frac{e_1 \wedge e_4 + e_2 \wedge e_3}{2}) \\ &= e_1 \wedge (x_1 e_2 + x_2 e_3 + x_3 e_4) \end{aligned} \tag{5.8}$$

where $x_3 \geq 0$ is the only restriction.

The result above shows what "red fibers" looks like on $S^3 \subset \mathbb{R}^4$: they are all the great circles on S^3 which run through point 1. Most of them counted with only one orientation (from 1 to $(x_1e_2 + x_2e_3 + x_3e_4)$ when $x_3 > 0$), except for those with $x_3 = 0$, which are $e_1 \wedge (x_1e_2 + x_2e_3)$ passing through $\langle \mathbf{i}, \mathbf{j} \rangle$ plane, with both orientations. This is exactly the theorem 5.1.1 part 1.

(2) "Blue fibers"

For the blue fibers, we will restrict f_s to the lower hemisphere $S^2_-\big|_L$ (subscript "L" means "lower"). Given any point $x \in S^2_-\big|_L$, similar to (5.5), it can be expressed with respect to the basis as

$$x = x_1 b_1^- + x_2 b_2^- - x_3 b_3^- \tag{5.9}$$

where $x_1^2 + x_2^2 + x_3^2 = 1$ and $x_3 \geq 0$.

With formula (5.1), we have

$$\begin{aligned} f_s(b_1^-) &= b_1^+ \\ f_x(b_2^-) &= b_2^+ \\ f_x(-b_3^-) &= b_3^+ \end{aligned} \tag{5.10}$$

and thus

$$f(x) = x_1 b_1^+ + x_2 b_2^+ + x_3 b_3^+ \tag{5.11}$$

Again, using formula (5.4), we can recover the original great circle fiber C_x corresponding to $(x, f(x))$ as

$$\begin{aligned}
C_x &= x + f(x) \\
&= x_1 b_1^- + x_2 b_2^- - x_3 b_3^- + x_1 b_1^+ + x_2 b_2^+ + x_3 b_3^+ \\
&= x_1(\frac{e_1 \wedge e_2 - e_3 \wedge e_4}{2}) + x_2(\frac{e_1 \wedge e_3 + e_2 \wedge e_4}{2}) - x_3(\frac{e_1 \wedge e_4 - e_2 \wedge e_3}{2}) \\
&\quad + x_1(\frac{e_1 \wedge e_2 + e_3 \wedge e_4}{2}) + x_2(\frac{e_1 \wedge e_3 - e_2 \wedge e_4}{2}) + x_3(\frac{e_1 \wedge e_4 + e_2 \wedge e_3}{2}) \\
&= x_1 e_1 \wedge e_2 + x_2 e_1 \wedge e_3 + x_3 e_2 \wedge e_3 \\
&= e_1 \wedge (x_1 e_2 + x_2 e_3) + x_3 e_2 \wedge e_3 \\
&= e_1 \wedge (x_1 e_2 + x_2 e_3) + \frac{x_3}{x_2} e_2 \wedge (x_1 e_2 + x_2 e_3) \\
&= (e_1 + \frac{x_3}{x_2} e_2) \wedge (x_1 e_2 + x_2 e_3) \qquad \text{(if } x_2 \neq 0\text{)}
\end{aligned} \tag{5.12}$$

where $x_1^2 + x_2^2 + x_3^2 = 1$ and $x_3 \geq 0$.

The result above shows what "blue fibers" looks like on $S^3 \subset \mathbb{R}^4$: They consist of all the great circles on $S^2(1, \mathbf{i}, \mathbf{j}) \subset S^3$, the unit two-sphere in the subspace $\mathbb{R}^3$ spanned by $1, \mathbf{i}, \mathbf{j}$. If $x_3 \neq 0$, the fiber C_x has only one orientation by the "right-hand rule". The right-hand rule means that imagine you are in the Euclidean space $\mathbb{R}^3 = \langle 1, \mathbf{i}, \mathbf{j} \rangle$, then curl the fingers of your right hand in the direction of the orientation of this blue great circle (from $(e_1 + \frac{x_3}{x_2} e_2)$ to $(x_1 e_2 + x_2 e_3)$) and your thumb must point in the direction of the upper half-space containing $\mathbf{j}$ instead of $-\mathbf{j}$. When $x_3 = 0$, this rule fails unambiguously and all the fibers go through the poles 1 and -1 of the two-sphere $S^2(1, \mathbf{i}, \mathbf{j})$, in which case they are counted with both orientations.

Remark. The last expression in the (5.12) requires $x_2 \neq 0$. If $x_2 = 0$ but $x_1 \neq 0$, we can used $C_x = (e_1 - \frac{x_3}{x_1} e_3) \wedge (x_1 e_2 + x_2 e_3)$ instead for visualizaiton. If $x_1 = x_2 = 0$, then $C_x = e_2 \wedge e_3$. Both cases confirm the theorem 5.1.1 part 2.

5.2.2. (3)"Orange fibers"

The "Orange fibers" correspond to the f_s restricted to the equator, which is the intersection of both "blue fibers" and "red fibers". In such case, x is simply $x_1 b_1^- + x_2 b_2^-$ and $C_x = e_1 \wedge (x_1 e_2 + x_2 e_3)$.

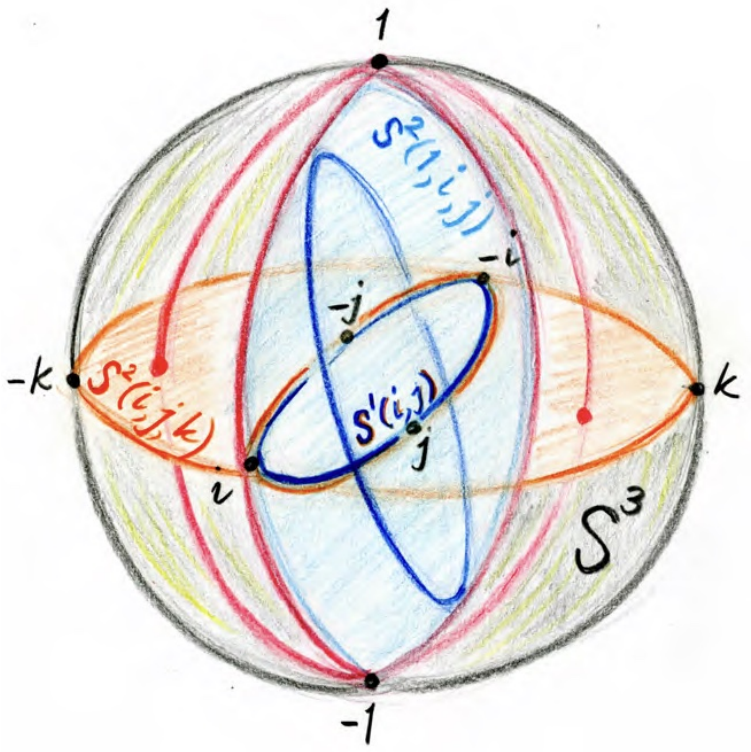

Figure 5.1: "Red", "Blue" and "Orange" fibers on the standard singular fibrations $\mathcal{S}$

This can be easily verified via direct computation as above or let $x_3 = 0$ in the equation (5.8) or (5.12).

Since the only restriction on x_1 and x_2 is $x_1^2 + x_2^2 = 1$, the fiber C_x has both two orientations and are two separate points in the base space of $\mathcal{S}$.

Finally, we show the figures of the standard singular fibrations, and how they lie in $\tilde{\mathrm{G}}_2\mathbb{R}^4$ as parts of two diagonals, repsectively. See Figure 5.1, Figure 5.2a and Figure 5.2b.

5.3. Dynamics of the standard singular fibration

In this section, we will describe how the standard singular fibration is formed through a path of (continuous) non-singular great circle fibraions on S^3. We will use the quaternion model to achieve the computation.

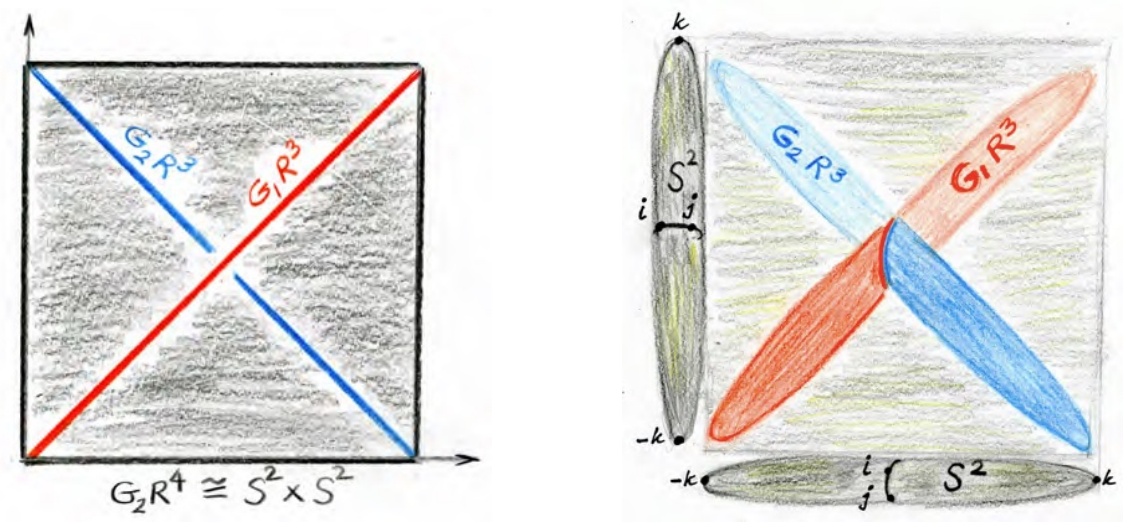

(a) (b)

Figure 5.2: "Red fibers" as the main diagonal $G_1\mathbb{R}^3$ and "blue fibers" as an anti-diagonal $G_2\mathbb{R}^3$

5.3.1. Formation of the singular fibration

Let's first define a specific path of continuous great circle fibrations that converges to the standard singular fibration $\mathcal{S}$.

Definition 5.3.1. A (canonical) path of continuous great circle fibrations, denoted as $\mathcal{F}_t$, converging to the standard singular fibration $\mathcal{S}$, is defined as the homotopy of the corresponding distance-decreasing maps f_t in either the exterior algebra model or the quaternion model (again, they are identical). Specifically, for any $x \in S^2_-$,

$$f_t(x) = \begin{cases} t \cdot \widehat{\mathbf{k}x} & \text{if } x \text{ in the upper hemisphere} \\ f_t(x^*) & \text{if } x \text{ in the lower hemisphere} \end{cases} \tag{5.13}$$

and $t \in [0, 1]$. Here, $\widehat{\mathbf{k}x}$ means the shortest geodesic (i.e. shortest arc of a great circle) connecting from $\mathbf{k}$, the north pole, to the point x, and $t \cdot \widehat{\mathbf{k}x}$ means the end point of the geodesic evenly shrunk from $\widehat{\mathbf{k}x}$ towards $\mathbf{k}$ by a multiplier t to the arc length (or equivalently to the radian).

Remark. It is worthwhile to point out that when $t = 1$, $f_t(x) = f_s(x)$, corresponding to the standard singular fibration $\mathcal{S}$ and when $t = 0$, $f_t(x) \equiv \mathbf{k}$, corresponding to the Hopf fibration containing $1 \wedge \mathbf{k}$

and $\mathbf{i} \wedge \mathbf{j}$. Therefore, this homotopy takes this Hopf fibration $\mathcal{F}_0$ continuously throught a path of great circle fibrations $\mathcal{F}_t$ to the standard singular fibration $\mathcal{F}_1 = \mathcal{S}$.

To understand this formation, let's focus on the most important subspace, the equatorial torus T_t of $\mathcal{F}_t$ and compute explicitly how it evolves as t grows from 0 to 1. The definition of T_t is

Definition 5.3.2. With the same notation as in 5.3.1, we restrict f_t to the equator S^1_e of S^2_-, then the map $f_t\big|_{S^1_e} : S^1_e \mapsto$ shrunk S^1_e will correspond to a circle worth of great circle fibres, and call it the equatorial torus T_t.

We have following very important oberservations directly from defintions and previous chapters:

1. When $t = 1$, T_t is the image of the diagonal map $D : S^1 \mapsto \tilde{\mathrm{G}}_2\mathbb{R}^4 \cong S^2 \times S^2$ to the equators of each S^2. This corresponds to the "orange fibers" in the standard singular fibration, consisting of all oriented fibers passing through 1 and intersecting with the plane $\langle \mathbf{i}, \mathbf{j} \rangle$.

2. When $t = 0$, T_t is exactly the equator of the space $S^2_- \times \{\mathbf{k}\}$, which correspond to the Hopf fibration in the remark above. Therefore, the total space of T_t in S^3 is exactly the *Clifford torus* in the middle of the three-shere.

3. When $0 < t < 1$, T_t will correspond to a path of *compressed* torus in the middle of S^3 as a subbundle of $\mathcal{F}_t$. They are not flat.

With these critical observations, we can visualize the homotopy f_t as the dynmaics of the formation of the standard singular fibration $\mathcal{S}$.

Specifically, we will use the *stereographic projection* to project this process into $\mathbb{R}^3 \cup \{\infty\}$.

Definition 5.3.3. The *stereographic projection* is a map $P : S^n \mapsto \mathbb{R}^n \cup \{\infty\}$. Let N denote the north pole $(0, \cdots, 0, 1)$ of $S^n \subset \mathbb{R}^{n+1}$ and $\mathbb{R}^n$ be identified with the hyperplane $\{x | x_{n+1} = 0\}$ in $\mathbb{R}^{n+1}$. Given any point $x = (x^1, \cdots, x^{n+1}) \in S^n \setminus \{N\}$, then $P(x)$ is the the point of intersection

of the line Nx with $\mathbb{R}^n$. In coordinates,

$$P(x) = \frac{(x^1, \cdots, x^{n+1})}{1 - x^{n+1}} \tag{5.14}$$

We let $P(N) := \infty$.

Now let's compute the coordinate of the image of T_t in $\mathbb{R}^3$ after stereographic projection. Recall that we will use the quaternion model in this computation.

Given any point $a \in S^1_e \subset S^2_-$ on the equator of the domain two-sphere, which can be represented as a unit pure imaganiry quaternion $a = \cos\theta\mathbf{i} + \sin\theta\mathbf{j}$ for $\theta \in [-\pi, \pi]$, we have that

$$f_t(a) = t \cdot \widehat{\mathbf{k}a} = \cos\frac{t\pi}{2}a + \sin\frac{t\pi}{2}\mathbf{k} \tag{5.15}$$

To visualize the transformation of T_t, we need to first recover its corresponding fibers in S^3. According to the Section 2.2, we have that the corresponding fiber of $(a, f_t(a))$ is $c_t \wedge c_t a$, where c_t is the midpoint of any geodesic arc connecting a and $f_t(a)$ on S^2. Therefore, we have

$$c_t = \cos\frac{t\pi}{4}a + \sin\frac{t\pi}{4}\mathbf{k} \tag{5.16}$$

Hence,

$$\begin{aligned} c_t a &= (\cos\frac{t\pi}{4}a + \sin\frac{t\pi}{4}\mathbf{k})a \\ &= -\cos\frac{t\pi}{4} - \sin\frac{t\pi}{4}a\mathbf{k} \end{aligned} \tag{5.17}$$

Therefore, we recover the fiber associated with $(a, f_t(a))$ as

$$c_t \wedge c_t a = (\cos\frac{t\pi}{4}a + \sin\frac{t\pi}{4}\mathbf{k}) \wedge (-\cos\frac{t\pi}{4} - \sin\frac{t\pi}{4}a\mathbf{k}) \tag{5.18}$$

and a point x on this fiber is

$$\begin{aligned} x &= \cos\varphi(\cos\frac{t\pi}{4}a + \sin\frac{t\pi}{4}\mathbf{k}) + \sin\varphi(-\cos\frac{t\pi}{4} - \sin\frac{t\pi}{4}a\mathbf{k}) \\ &= \cos\varphi(\cos\frac{t\pi}{4}(\cos\theta\mathbf{i} + \sin\theta\mathbf{j}) + \sin\frac{t\pi}{4}\mathbf{k}) \\ &\quad + \sin\varphi(-\cos\frac{t\pi}{4} - \sin\frac{t\pi}{4}(\cos\theta\mathbf{i} + \sin\theta\mathbf{j})\mathbf{k}) \\ &= -\sin\varphi\cos\frac{t\pi}{4} + (\cos\varphi\cos\frac{t\pi}{4}\cos\theta - \sin\varphi\sin\frac{t\pi}{4}\sin\theta)\mathbf{i} \\ &\quad + (\cos\varphi\cos\frac{t\pi}{4}\sin\theta + \sin\varphi\sin\frac{t\pi}{4}\cos\theta)\mathbf{j} + \cos\varphi\sin\frac{t\pi}{4}\mathbf{k} \end{aligned} \tag{5.19}$$

where $\varphi \in [-\pi, \pi]$.

If we write this in the Euclidean coordinate, we finally have the coordinate for a general point $x \in T_t$,

$$\begin{aligned} x = \big(&-\sin\varphi\cos\frac{t\pi}{4},\ \cos\varphi\cos\frac{t\pi}{4}\cos\theta - \sin\varphi\sin\frac{t\pi}{4}\sin\theta, \\ &\cos\varphi\cos\frac{t\pi}{4}\sin\theta + \sin\varphi\sin\frac{t\pi}{4}\cos\theta,\ \cos\varphi\sin\frac{t\pi}{4}\big) \end{aligned} \tag{5.20}$$

Next, we will apply the stereographic projection onto this point x, which gives the deserved visual representative point $P(x)$ as

$$\begin{aligned} P(x) = \Bigg(&\frac{-\sin\varphi\cos\frac{t\pi}{4}}{1-\cos\varphi\sin\frac{t\pi}{4}},\ \frac{\cos\varphi\cos\frac{t\pi}{4}\cos\theta - \sin\varphi\sin\frac{t\pi}{4}\sin\theta}{1-\cos\varphi\sin\frac{t\pi}{4}}, \\ &\frac{\cos\varphi\cos\frac{t\pi}{4}\sin\theta + \sin\varphi\sin\frac{t\pi}{4}\cos\theta}{1-\cos\varphi\sin\frac{t\pi}{4}}\Bigg) \end{aligned} \tag{5.21}$$

Finally, we use the MATLAB to make the animation to show how the T_t look like in $\mathbb{R}^3$ and how it gradually tansforms from the Clifford torus to the "singular" two-sphere $S^2(1, i, j)$. See Figure 5.3.

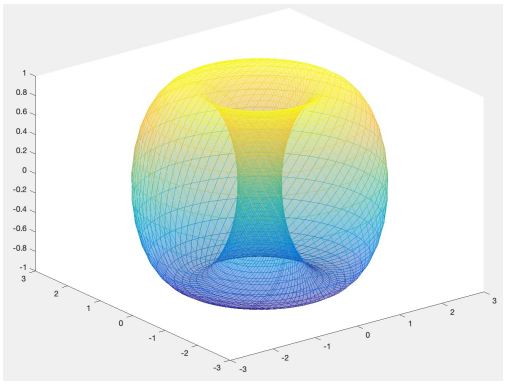

(a) Clifford torus inside of a Hopf fibraiton

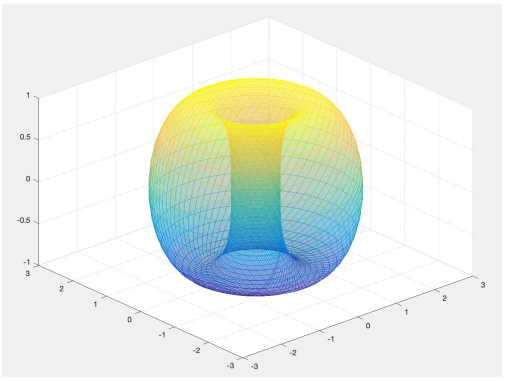

(b) $T_{0.2}$

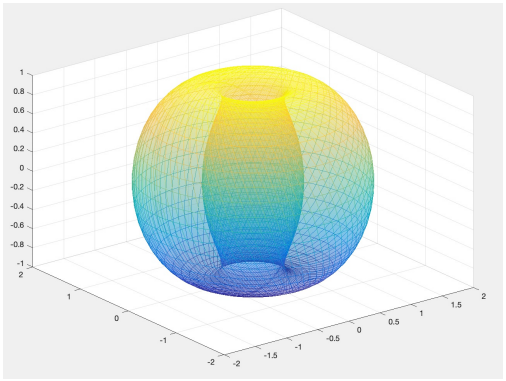

(c) $T_{0.4}$

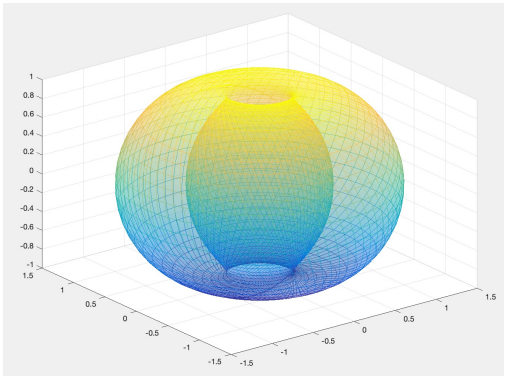

(d) $T_{0.6}$

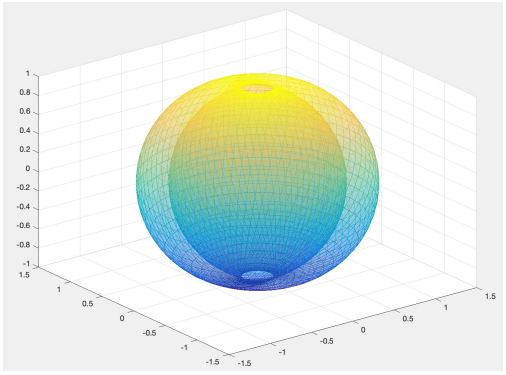

(e) $T_{0.8}$

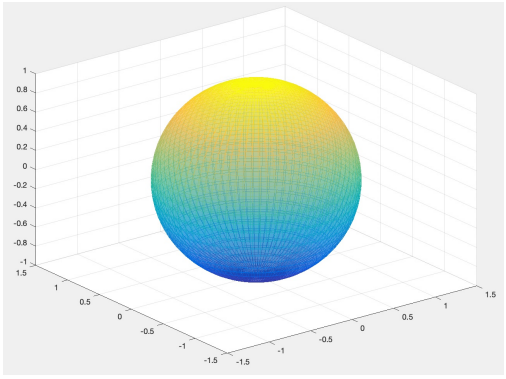

(f) singular sphere in the standard singular fibration

Figure 5.3: The development of T_t

CHAPTER 6

SMOOTH APPROXIMATION OF SINGULAR GREAT CIRCLE FIBRATIONS OF S^3

6.1. Introduction

In the previous chapter, we see how a typical singular fibration can be developed continuously through a path of non-singular fibrations. However, each of these non-singular fibrations is not differentiable. This is because the folding point on the equator is too "sharp" such that the change of the velocity when you move from the south pole to the north pole of the domain sphere will break when you pass the equator.

This incites us to prove the main theorem of this chapter.

Theorem 6.1.1 (Smooth Approximation)**.** *The smooth non-singular great circle fibrations of the three-sphere are dense in the continuous ones in the compact-open topology, and therefore dense in the moduli space of general great circle fibrations $\mathcal{SG}$.*

In another word, any great circle fibration of S^3, including singular fibrations, can be approximated by a sequence of smooth regular great circle fibrations.

In the second section, we will prove this theorem in the following steps:

1. Convert the question of "smooth approximation of the fibrations" into the question of "smooth approximation of Lipschitz maps",

2. Change the spherical metric on S^2 to the Euclidean straight-line metric and construct a smooth approximation in the $\mathbb{R}^3$,

3. Project back to the sphere S^2.

Since the proof involves many important technical details which may distract us from understanding the core ideas, we will move the proof for these details to the last section.

6.2. Smooth approximation

In this section, we will give a complete proof of the main theorem 6.1.1 in this chapter, putting off many important technical details to the next section, such that the flow of reasoning will not be interrupted.

Before we give the proof, let's first give a quick introduction on *Lipschitz maps* and some useful conventions. Recall the definition of Lipschitz continuity:

Definition 6.2.1. Given two metric spaces (X, d_X) and (Y, d_Y), where d_X, d_Y denote the metrics on the spaces X and Y, a function $f : X \mapsto Y$ is called *Lipschitz (continuous)* if there exists a real constant $K \geq 0$ such that, for all x_1 and x_2 in X, $d_Y(f(x_1), f(x_2)) \leq K \cdot d_X(x_1, x_2)$. The smallest such K will be called *the Lipschitz constant of* f.

Note that f is distance-decreasing (weakly or strictly) is equivalent to the condition that the Lipschitz constant of f is not bigger than 1.
Since we will benefit from two different metrics or distance functions on S^2 to give constructive proof of this theorem, let's make some important conventions for clarity. Specifically, denote the Euclidean straight-line distance and the induced spherical distance as $e(x, y)$ and $d(x, y)$ for $x, y \in S^2 \subset \mathbb{R}^3$,

$$e(x, y) = \|x - y\|$$

and

$$d(x, y) = \inf\{L(\lambda)\text{: } \lambda \text{ a piecewise continuously differentiable curve from } x \text{ to } y \text{ on } S^2\}$$

and call the corresponding Lipschitz constants K_e and K_d.
We will also use subscripts to distinguish the domain two-sphere S^2_- and the codomain two sphere S^2_+ if necessary. Now we are ready to give the proof of the main theorem 6.1.1.

Proof. Given any continuous great circle fibration F, let's denote its corresponding continuous map

on S^2 as $f : S^2 \mapsto S^2$. Then we have $K_d(f) \leq 1$ and according to Chapter 4, the image of f will be contained in a hemisphere. Our goal is to construct an arbitrarily close smooth $f' : S^2 \mapsto S^2$ with Lipschitz constant $K_d(f') < 1$ such that it corresponds to a smooth non-singular great circle fibration.

First, we switch to the Euclidean distance function on S^2. According to the lemma 6.3.5 in the next section, $K_e(f) \leq 1$ as well. Then we shrink the image of f in the hemisphere towards its center such that the shrunk f_s staying ϵ close to the original map f, where ϵ is arbitrarily small, then by lemma 6.3.7, the Lipschitz constant $K_e(f_s)$ is strictly smaller than 1. Let's assume $K_e(f_s) \leq 1 - \delta(\epsilon)$ where $\delta(\epsilon)$ depending on ϵ is positive. This new map, f_s, gives us a little room $\delta(\epsilon)$ for its Lipschitz constant from 1 but keeps ϵ close to the original map f. If we can approximate this new map f_s arbitrarily close (say within ϵ uniform neighborhood) by a smooth one with a very close Lipschitz constant (probably bigger but still bounded by a number strictly smaller than 1), then it will correspond to a smooth great circle fibration which is very close to the original one (less than 2ϵ), which proves the main theorem. Let's elaborate above process carefully in steps.

(1) By *Kirszbraun's Theorem* (6.3.8), we are able to extend this shrunk $f_s : S^2 \mapsto S^2 \subset \mathbb{R}^3$ to a new map $\bar{f} : \mathbb{R}^3 \mapsto \mathbb{R}^3$, with the same Euclidean Lipschitz constant $K_e(\bar{f}) = K_e(f_s) \leq 1 - \delta(\epsilon) < 1$. Notice that we are in the category of the straight-line metric now.

(2) According to the important lemma 6.3.9, we can use convolution with a smooth kernel function to uniformly approximate (in Euclidean distance) $\bar{f}$ with a smooth map $g : \mathbb{R}^3 \mapsto \mathbb{R}^3$, and both of them have the same Lipschitz constant $K_e(g) = K_e(\bar{f})$. We will choose the map g such that its image $g(x)$ is uniformly closed to $\bar{f}(x)$, say within an undecided $\tilde{\epsilon}$ neighborhood of $\bar{f}(x)$ in $\mathbb{R}^3$ for each x, where the explicit scale of $\tilde{\epsilon}$ will be confirmed in the step **(3)**. We restrict g to S^2 and also denote it as $g : S^2 \mapsto \mathbb{R}^3$ for simplicity. Notice that its Euclidean Lipschitz constant may be even smaller after restriction but we will not take advantage of this.

(3) Finally, we project $g(S^2)$ Orthogonally (along the radius connecting the origin and $g(x)$) back to the original codomain S^2 and call this new map $f' : \mathbb{R}^3 \mapsto S^2$. Notice that this step will (sometimes)

increase both the distance of the image (i.e. $d(f'(x), f(x)) \geq e(g(x), f(x))$) and the Euclidean Lipschitz constant (i.e. $K_e(f') \geq K_e(g)$). However, fortunately, this can be easily controlled by selecting a very small $\tilde{\epsilon}$ in the previous step **(2)**, such that the whole image of $g(x)$ is very close to the two-sphere (lying in the tubular neighborhood of radius $\tilde{\epsilon}$). In this way, the projection within such a small tubular neighborhood will only increase its Euclidean Lipschitz constant $K_e(f')$ by a small amount such that $K_e(f')$ is still strictly less than 1 (even if it may be bigger than $K_e(g)$, this will work since we shrink f at the beginning to have some room), and increase its uniform distance from the original map f by less than ϵ as well.

Finally, we have this smooth map $f' : S^2 \mapsto S^2$, when is at most 2ϵ uniformly far away from the original map f by our construction, and will have $k_d(f') \leq k_e(f') < 1$ according to the lemma. Since $k_d(f')$ implies $|df'| < 1$, it will correspond to a smooth fibration F' of S^3 by oriented great circles which is uniformly close to the original continuous fibration F corresponding f. This completes the proof. □

6.3. Proof of related lemmas

We will follow the same notation as in the last section. Specifically, $f : S^2 \mapsto S^2$ is a continuous map between two unit $S^2 \subset \mathbb{R}^3$, and we use $e(x, y)$ and $d(x, y)$ to represent Euclidean straight-line distance and the standard spherical distance on S^2 respectively. $K_e(f)$ and $K_d(f)$ are Lipschitz constants of f in these two metrics. Let's give some definitions and fundamental results on the Lipschitz maps first. We won't prove this because they are standard in any analysis book.

Definition 6.3.1. If $U \in S^2$ is a subset, then we can also consider the Lipschitz constant of the restriction $f|_U$, which will be written as $K_e(f, U)$ or $K_d(f, U)$, depending on the metric to work with, and regard it as the *local Lipschitz constant of f on U*.

Definition 6.3.2. Given a sequence $\{U_i\} := U_1 \supset U_2 \supset ... \supset U_n \supset ...$ of decreased open subsets of S^2 containing a point $x \in S^2$. It is said that $\{U_i\}$ *converges to x* if, given any open subset U containing x, there is an integer n such that $U \subset U_n$. Then the Lipschitz constants $K(f, U_n)$ must decrease as n increases. We call their limit *the Lipschitz constant of f at x*, and write it as $K(f, x)$.

It is well-defined since it does not depend on which sequence of open sets $\{U_i\}$ converging to x we use.

Lemma 6.3.1. $K_d(f) = \sup\{K_d(f,x) \ : \ x \in S^2\}$

Lemma 6.3.2. $K_e(f) >= \sup\{K_e(f,x) \ : \ x \in S^2\}$

Lemma 6.3.3. $K_e(f,x) = K_d(f,x)$ *for any* $x \in S^2$

Lemma 6.3.4. *Given an open covering* $\mathcal{C} = \{U_\alpha\}$ *of* S^2 *and that on each open set* U_α, f *is Lipschitz with Lipschitz constant* $K_d(f, U_\alpha)$. *Then* f *is Lipschitz with Lipschitz constant* $K_d(f) = \max\{K_d(f, U_\alpha) : U_\alpha \in \mathcal{C}\}$

Remark (1). All of the above lemmas are standard: 6.3.1, 6.3.2, 6.3.4 can be shown directly with the proof by contradiction. 6.3.3 is from the fact that the spherical metric is induced from the Euclidean inner product, and thus they are locally identical in an infinitesimal neighborhood.

Remark (2). All of the definitions and lemmas can be generalized to arbitrary map $f : X \mapsto Y$ between two metric spaces, where d and e are "pathwise metric" and "induced metric" from ambient metric spaces $X \subset \tilde{X}$ and $Y \subset \tilde{Y}$.

Next, we will list and prove important lemmas used in the proof of the main theorem in the last section.

Lemma 6.3.5. $K_d(f) \leq 1 \Leftrightarrow K_e(f) \leq 1$.

Proof. Given any two points $x, y \in S^2$, let $d(x,y) = \theta_{x,y}$. Then $e(x,y) = 2\sin(\theta_{x,y}/2)$, the length of the chord connecting x and y. Since $2\sin(\theta/2)$ is strictly monotonic function with respect to θ,

we have

$$
\begin{aligned}
& K_d(f) \leq 1 \\
& \Leftrightarrow d(f(x), f(y)) \leq d(x, y) \\
& \Leftrightarrow \theta_{f(x),f(y)} \leq \theta_{x,y} \\
& \Leftrightarrow 2\sin(\theta_{f(x),f(y)}/2) \leq 2\sin(\theta_{x,y}/2) \\
& \Leftrightarrow e(f(x), f(y)) \leq e(x, y) \\
& \Leftrightarrow K_e(f) \leq 1
\end{aligned}
$$

□

Lemma 6.3.6. $K_d(f) \leq K_e(f)$

Proof. This can be verified directly from the previous lemmas. In fact, we have that

$$
\begin{aligned}
k_d(f) &= \sup\{K_d(f, x) \ : \ x \in S^2\} && \text{(Lemma 6.3.1)} \\
&= \sup\{K_e(f, x) \ : \ x \in S^2\} && \text{(Lemma 6.3.3)} \\
&\leq K_e(f) && \text{(Lemma 6.3.2)}
\end{aligned}
$$

□

Lemma 6.3.7. *Given that the image of $f : S^2 \mapsto S^2$ is contained in a hemisphere centered at p, if we shrink the image of f in the hemisphere towards the center p along the geodesic towards p by a scale $1 - \delta$, where $\delta > 0$ is a small number, and denote the new shrunk map as f_s, then $K_d(f_s) < K_d(f)$ and $K_e(f_s) < K_e(f)$.*

Proof. This is standard computation. □

Next, we will introduce a strong and useful result from Kirszbraun, which guarantees a Lipschitz extension of $f : S^2 \mapsto S^2$ to the whole space $F : \mathbb{R}^3 \mapsto \mathbb{R}^3$.

Theorem 6.3.8 (Kirszbraun)**.** *If U is a subset of some Hilbert space H_1 with the subsapce metric, and H_2 is another Hilbert space, and $f : U \mapsto H_2$ is a Lipschitz-continuous map with Lipschitz constant $L(f, U)$, then there is a Lipschitz-continuous map $F : H_1 \mapsto H_2$ that extends f and has the same Lipschitz constant $L(f, U)$.*

Proof. (simplest case) Assume H_2 is $\mathbb{R}$ the real line, we can define

$$F(x) = \inf_{u \in U} (f(u) + L(f, U) \cdot d(x, u))$$

□

Remark. When $H_2 = \mathbb{R}^m$, Daniel Azagra et al.(2021) give another explicit extension formula. More general proof can be found in the book.

Next, We will prove a very important lemma, which is the *smooth approximation of Lipschitz maps between Euclidean spaces.* This lemma helps us to convert a non-smooth Lipschitz map to a smooth one in the main proof.

Lemma 6.3.9. *Any continuous map $f : \mathbb{R}^n \mapsto \mathbb{R}^m$ between two Euclidean spaces (both of standard Euclidean metrics) with Lipschitz constant L can be approximated uniformly by a smooth Lipschitz map with the same Lipschitz constant L.*

Proof. We will give constructive proof using convolution with a smooth kernel.
(Smoothness) First, define $j : \mathbb{R} \mapsto \mathbb{R}$ as follows

$$j(x) = \begin{cases} e^{-\frac{1}{x^2}} & \text{if } x > 0 \\ 0 & \text{if } x \leq 0 \end{cases} \tag{6.1}$$

$j(x) \in C^\infty(\mathbb{R})$ is a smooth function.

Then we can define a smooth function $h : \mathbb{R}^n \mapsto \mathbb{R}$ from $j(x)$

$$h(x) = cj(1 - \|x\|^2), \quad \text{for } x \in \mathbb{R}^n$$

where $c > 0$ is the constant such that

$$\int_{\mathbb{R}^n} h(x)dx = 1$$

Notice that $h(x) \in C^\infty(\mathbb{R}^n)$, $h(x) \geq 0$ and supp $h \subset \mathrm{B}_1(0)$, the unit ball at 0.

Let's define the mollifier,

$$h_\epsilon(x) = \frac{1}{\epsilon^n} h(\frac{x}{\epsilon})$$

Then it's also true that

$$\int_{\mathbb{R}^n} h_\epsilon(x)dx = 1$$

. Let f_ϵ be the entry-wise convolution of f by the mollifier h_ϵ. Specifically,

$$\begin{aligned} f_\epsilon &= (f_\epsilon^1, f_\epsilon^2, \cdots, f_\epsilon^m) \\ &= f * h_\epsilon \\ &:= (f^1 * h_\epsilon, f^2 * h_\epsilon, \cdots, f^m * h_\epsilon) \end{aligned} \tag{6.2}$$

where each entry

$$\begin{aligned} f_\epsilon^i(x) &= f^i * h_\epsilon(x) \\ &= \int_{\mathbb{R}^n} f^i(y) h_\epsilon(x - y)dy \\ &= \int_{\mathbb{R}^n} f^i(x - y) h_\epsilon(y)dy && \text{(change of variable } y = x - y) \\ &= \frac{1}{\epsilon^n} \int_{\mathrm{B}_\epsilon(0)} f^i(x - y) h(\frac{y}{\epsilon})dy && \text{(definition of } h_\epsilon) \\ &= \int_{\mathrm{B}_1(0)} f^i(x - \epsilon y) h(y)dy && \text{(change of variable } y = \epsilon y) \end{aligned} \tag{6.3}$$

Then f_ϵ is a C^∞ map because convolution will regularize the map f. Next, we will estimate the Lipschitz constant of f_ϵ.

(Lipschitz constant) For any pair of distinct points $x_1, x_2 \in \mathbb{R}^n$, we have that

$$f_\epsilon(x_1) - f_\epsilon(x_2) = \Big(\int_{\mathbb{R}^n} (f^i(x_1 - y) - f^i(x_2 - y)) h_\epsilon(y) dy \Big)_{i=1,\cdots,m} \tag{6.4}$$

on the right-hand side, we use subscript "$i = 1, \cdots, m$" to stand for each coordinate i.

For simplicity, let's denote

$$g^i(y) := f^i(x_1 - y) - f^i(x_2 - y) \tag{6.5}$$

and

$$g(y) := (g^1(y), g^2(y), \cdots, g^m(y)) = f(x_1 - y) - f(x_2 - y) \tag{6.6}$$

Consider an arbitrary random vector Y from some probability space $(\Omega, \mathcal{F}, P)$ to $\mathbb{R}^n$ with the probability distribution as

$$Y \ \sim \ h_\epsilon(y) dy \quad \text{on} \quad \mathbb{R}^n \tag{6.7}$$

We denote $Z^i := g^i(Y)$ as another random variable. Then

$$Z := (Z^1, \cdots, Z^m) = (g^1(Y), \cdots, g^m(Y)) = g(Y) \tag{6.8}$$

is a random vector. In this setting of probability and measure theory, we have that

$$\begin{aligned}
&\mathbb{E}\, Z \\
&:= (\ \mathbb{E}\, Z^i\ )_{i=1,\cdots,m} \\
&= \left(\int_\Omega g^i(Y) dP \right)_{i=1,\cdots,m} \\
&= \left(\int_{\mathbb{R}^n} g^i(y) h_\epsilon(y) dy \right)_{i=1,\cdots,m} \\
&= f_\epsilon(x_1) - f_\epsilon(x_2) \qquad\qquad (\ 6.4 \text{ and } 6.5\ )
\end{aligned} \tag{6.9}$$

Now we can take advantage of the *Jensen's inequality* to make an estimate on the norm of $\|f_\epsilon(x_1) - f_\epsilon(x_2)\|$.

Lemma (*Jensen's inequality*) *Let f be a convex function defined on a convex subset C of n-dimensional Euclidean space $\mathbb{R}^n$, and let $X = (X_1, \cdots, X_n)$ be an integrable random vector such that $\mathbb{P}[X \in C] = 1$. Then $\mathbb{E}\, X \in C$, $\mathbb{E}\, f(X)$ exits, and*

$$f(\mathbb{E}\, X) \leq \mathbb{E}\, f(X). \tag{6.10}$$

The proof of this inequality is standard in any analysis book.

In our case, let $f = \|\cdot\|^2$ be the squared Euclidean norm and $X = Z$. Since the squared Euclidean norm is a convex function, we have

$$\begin{aligned}
&\|f_\epsilon(x_1) - f_\epsilon(x_2)\|^2 \\
&= \|\,\mathbb{E}\, Z\|^2 && (6.8)\\
&\leq \mathbb{E}\,\|Z\|^2 && \text{Jensen's inequality (6.10)}\\
&= \mathbb{E}\,\|g(Y)\|^2 && (6.8)\\
&= \int_\omega \|g(Y)\|^2 dP && \text{Definition of expectation}\\
&= \int_{\mathbb{R}^n} \|g(y)\|^2\ h_\epsilon(y)dy \\
&= \int_{\mathbb{R}^n} \|f(x_1 - y) - f(x_2 - y)\|^2 h_\epsilon(y)dy && (6.6)\\
&\leq \int_{\mathbb{R}^n} L^2\|x_1 - x_2\|^2 h_\epsilon(y)dy && \text{Lipschitz continuity}\\
&= L^2\|x_1 - x_2\|^2
\end{aligned} \tag{6.11}$$

This proves that $f_\epsilon(x)$ is also Lipschitz with the Lipschitz constant L, the same as f's.

(Uniform approximation) Finally, let's estimate the uniform distance between f_ϵ and f. We will use a similar strategy as above. Specifically, For any fixed $x \in \mathbb{R}^n$, let's consider an arbitrary random vector Y' from some probability space $(\Omega, \mathcal{F}, P)$ to $\mathbb{R}^n$ with the probability distribution as $Y' \sim h(y')dy'$ on $\mathbb{R}^n$ and define $Z' = f(x - \epsilon Y') - f(x)$, a random vector to $\mathbb{R}^m$.

Analogous to 6.9, we have

$$
\begin{aligned}
&\mathbb{E}\, Z' \\
&= \Big(\mathbb{E}(f^i(x-\epsilon Y') - f^i(x))\Big)_{i=1,\cdots,m} \\
&= \left(\int_\Omega \big(f^i(x-\epsilon Y') - f^i(x)\big) dP\right)_{i=1,\cdots,m} \\
&= \left(\int_{\mathrm{B}_1(0)} \big(f^i(x-\epsilon y') - f^i(x)\big) h(y') dy'\right)_{i=1,\cdots,m} && (\text{supp } h \subset \mathrm{B}_1(0)) \\
&= \Big(f^i_\epsilon(x) - f^i(x)\Big)_{i=1,\cdots,m} && \text{According to (6.3)} \\
&= f_\epsilon(x) - f(x)
\end{aligned}
\tag{6.12}
$$

Therefore, we have

$$
\begin{aligned}
&\|f_\epsilon(x) - f(x)\|^2 \\
&= \|\,\mathbb{E}\, Z'\|^2 \\
&\le \mathbb{E}\,\|Z'\|^2 && \text{Jensen's inequality (6.10)} \\
&= \mathbb{E}\,\|f(x-\epsilon Y') - f(x)\|^2 \\
&\le \epsilon^2 L^2\, \mathbb{E}\,\|Y'\|^2 && \text{Lipschitz continuity} \\
&\le \epsilon^2 L^2
\end{aligned}
\tag{6.13}
$$

The last inequality above is becuase $Y' \sim h(y')dy'$ on $\mathbb{R}^n$ and supp $h \subset \mathrm{B}_1(0)$, and thus $\mathbb{P}(\|Y'\|^2 \le 1) = 1$.

Since L is a fixed constant and ϵ can be chosen arbitrarily small, we proved that f_ϵ can uniformly approximate f with the same Lipschitz constant l, which concludes the proof of the lemma. $\square$

BIBLIOGRAPHY

Daniel Azagra, Juan Ferrera, Fernando López-Mesas, and Yenny Rangel. Smooth approximation of lipschitz functions on riemannian manifolds. *Journal of Mathematical Analysis and Applications*, 326(2):1370–1378, 2007.

Daniel Azagra, Erwan Le Gruyer, and Carlos Mudarra. Kirszbraun's theorem via an explicit formula. *Canadian Mathematical Bulletin*, 64(1):142–153, 2021.

Patricia Cahn, Herman Gluck, and Haggai Nuchi. Deformation and extension of fibrations of spheres by great circles. *arXiv preprint arXiv:1502.03428*, 2015.

Dennis DeTurck, Herman Gluck, Rafal Komendarczyk, Paul Melvin, Clayton Shonkwiler, and David Shea Vela-Vick. Pontryagin invariants and integral formulas for milnor's triple linking number. *arXiv preprint arXiv:1101.3374*, 2011.

Dennis DeTurck, Herman Gluck, Leandro Lichtenfelz, Mona Merling, Jingye Yang, and Yi Wang. Deformation retraction of the group of strict contactomorphisms of the three-sphere to the unitary group. *arXiv preprint arXiv:2108.08961*, 2021.

Herman Gluck and Frank W Warner. Great circle fibrations of the three-sphere. *Duke Math. J.*, 50 (1):107–132, 1983.

Herman Gluck and Jingye Yang. Great circle fibrations and contact structures on odd-dimensional spheres. *arXiv preprint arXiv:1901.06370*, 2019.

Robert E Greene and Hung-hsi Wu. c^∞ convex functions and manifolds of positive curvature. 1976.

Allen Hatcher. *Algebraic Topology*. Cambridge University Press, 2002.

M Lee John. Introduction to smooth manifolds, 2012.

Mojzesz Kirszbraun. Üon contracting and lipschitzian transformations. *Fundamenta Mathematicae*, 22(1):77–108, 1934.

Jean-Michel Lasry and Pierre-Louis Lions. A remark on regularization in hilbert spaces. *Israel Journal of Mathematics*, 55:257–266, 1986.

John M Lee. *Introduction to Riemannian manifolds*, volume 2. Springer, 2018.

EJ McShane. Extension of range of functions. *Bulletin of the American Mathematical Society*, 40 (12):837–842, 1934.

John Willard Milnor and James D Stasheff. *Characteristic classes*. Number 76. Princeton university

press, 1974.

Michael D Perlman. Jensen's inequality for a convex vector-valued function on an infinite-dimensional space. *Journal of Multivariate Analysis*, 4(1):52–65, 1974.

Jacob T Schwartz. *Nonlinear functional analysis*, volume 4. CRC Press, 1969.

Norman Steenrod. *The topology of fibre bundles*, volume 27. Princeton university press, 1999.